Design of superhydrophobic ultraoleophobic NyCo

Hoon Joo Lee · Jeffery R. Owens

Abstract The apparent contact angles of dodecane droplets deposited on a 50:50 nylon:cotton blended woven fabric (NyCo) were measured, and the characteristics required for an ultraoleophobic surface were described. The metastable Cassie–Baxter model, a transition status from the original Cassie–Baxter model to the Wenzel model, was investigated to design ultraoleophobic surfaces and to understand the wetting behavior of such surfaces. Using chemical and geometrical modifications of NyCo, a surface having contact angles to dodecane of greater than 150° and water contact angles of greater than 165° has been prepared. Good agreement between the predicted and measured contact angles was obtained. Developing a superhydrophobic ultraoleophobic material has been achieved by two criteria: a low-surface-energy and a properly designed surface morphology.

Introduction

Surface modification of soft materials has recently gained a great deal of interest from both academia and industry. This technology often changes surface energy, structure, morphology, wettability, and other physical properties of the materials [1, 2]. In order to determine the aging process of composite materials, the long-term wetting behavior of surfaces is often characterized by measuring water contact angles [3, 4]. Recently, the wetting behavior of soft materials has been studied intensively using nanotechnology and bio-mimicry. This interest extends beyond the bio-inspired, lotus leaf property of superhydrophobicity to materials that exhibit similar properties to oils, thus dubbed ultraoleophobic properties. The applications of such materials are far reaching and include medical clothing, protective gear, and high performance technical textiles [5–10].

A surface with a water contact angle exceeding 150° and a roll-off angle lower than 5° is called a superhydrophobic surface [11]. We define a surface with an oil contact angle over 150° as an ultraoleophobic surface, since not all surfaces having high contact angle to liquids have liquids roll off the surfaces unless a solid has a very low-surface-tension which is approximately a quarter of the surface tension of a liquid, i.e., although oil contact angle exceeds 150° on a highly oleophobic rough surface, oil does not rolls around when the surface is tilted but pins to the surface unless the Young contact angle, a contact angle on a smooth surface, is greater than 90°. Since the wettability of a solid surface is determined by two parameters, the chemical composition and the geometrical structure of a rough surface, the combination of these two factors can be used for the development of a superhydrophobic and ultraoleophobic surface [12–16].

In order to design a superhydrophobic ultraoleophobic surface, two predominant rough wetting models are used: the Wenzel model and the Cassie–Baxter model. In the Wenzel model, a liquid fills the grooves of a rough surface and completely wets the surface, while in the Cassie–Baxter model, a liquid sits on top of the surface and repels the liquid. To create a Cassie–Baxter surface, the Young contact angle of a liquid, θ_e, must be greater than 90° [17]. Analysis of the Cassie–Baxter model for assessing feasibility of ultraoleophobicity yields Eq. 1 from our previous research [6]:

H. J. Lee (✉)
College of Textiles, North Carolina State University,
2401 Research Drive, Raleigh, NC 27695, USA
e-mail: hoonjoo_lee@ncsu.edu

J. R. Owens
Air Force Research Laboratory, RXQL, 139 Barnes Drive,
Building 1117, Tyndall Air Force Base, FL 32403, USA

$$\gamma_L(1 + \cos\theta_e) = \gamma_L^d(1 + \cos\theta_e) + \gamma_L^p(1 + \cos\theta_e)$$
$$+ \gamma_L^H(1 + \cos\theta_e)$$
$$= 2\left(\sqrt{\gamma_S^d \cdot \gamma_L^d} + \sqrt{\gamma_S^p \cdot \gamma_L^p} + \sqrt{\gamma_S^H \cdot \gamma_L^H}\right)$$

Since the surface tensions of dodecane and most polymeric surfaces are determined by London dispersion forces, this equation can be simplified to:

$$\gamma_L(1 + \cos\theta_e) = 2\sqrt{\gamma_S \cdot \gamma_L} \qquad (1)$$

substituting $\gamma_L = 25.4$ dyne/cm for dodecane into Eq. 1 suggests γ_S must be smaller than 6.35 dyne/cm, and a smooth surface having $\gamma_S \le 6.35$ dyne/cm can be oleophobic ($\theta_e > 90°$). Since most solid surfaces typically possess $\gamma_S > 6.35$ dyne/cm, the Cassie–Baxter model does not allow for permanent ultraoleophobicity under normal circumstances. On a metastable Cassie–Baxter surface, a liquid initially sits on top of the surface due to the minimization of surface energy caused by air pockets inside the grooves of the rough surface. However, the liquid is drawn into contact with the rough surface over time, with the time to absorption being dependent on the surface tension and volume of the liquid, and the surface tension and surface morphology of the solid. Hence, an ultraoleophobic surface can be produced by designing a metastable Cassie–Baxter surface.

In this research, we create a metastable ultraoleophobic surface via chemical and geometrical modification. We reduced the surface energy of the fibers by grafting 1,1,2,2,-tetrahydrodecyltrimethoxysilane (fluorosilane) onto the fibers. We control macro scale roughness of the NyCo via choice of fabric weave, fiber diameter and using multifilament yarns. Additionally, we achieve micro and nano scale roughness on the fibers by allowing partial condensation of the fluorosilane prior to treating the NyCo, thus resulting in deposition of fluorosilane particulate condensates over the fiber surface.

Experimental

Materials

Nylon 6,6 film (M_n: 12 kDa) and NyCo (50:50 nylon 6,6/cotton blended) were used as smooth or rough surfaces. Fluorosilane ($C_{13}H_{13}F_{17}O_3Si$, Gelest, Morrisville, PA, USA), tetramethyl orthosilicate (TMOS, $SiC_4H_{12}O_4$, Aldrich), ammonium hydroxide (NH_4OH, Mallinckrodt Chemical, Raleigh, NC, USA), methanol (CH_3OH, Aldrich), and isopropyl alcohol (C_3H_7OH, Fisher) were used without further purification. Distilled water and dodecane ($C_{12}H_{26}$, Aldrich) were used as liquids to measure contact angles.

Grafting of fluorosilane on nylon film

In order to model a superhydrophobic ultraoleophobic surface, the Young contact angles, θ_e, of water and dodecane on a smooth surface covered by fluorosilane are required. Hence, fluorosilane was grafted to a nylon film. An aliquot of 0.1 g of fluorosilane was dissolved in 10 mL methanol at 20 °C. Then, 0.5 g of nylon film (10×10 cm^2) was immersed in the fluorosilane solution for 30 min, dried at 120 °C for 1 min, and cured at 170 °C for 2 min. The fluorosilane-grafted nylon film was rinsed in methanol for 2 h, wiped with Kimwipes®, and air dried.

Grafting of fluorosilane on NyCo

In order to provide micro and nano scale protuberances made of fluorosilane on the NyCo surface, we added 1% ammonium hydroxide to 10% fluorosilane solution in isopropyl alcohol and allowed partial condensation of the fluorsilane prior to treating the NyCo. A 3 g NyCo fabric (10×10 cm^2) was immersed in the prepared solution, padded to remove excess liquid, and cured in a microwave oven (Panasonic NN-SD967S) at 2.45 GHz/1.25 kW for 30 s (repeated thrice with fresh solution). The fluorosilane-grafted NyCo was rinsed in isopropyl alcohol and water for 2 h and air dried. Scheme 1 shows the conceptual reaction mechanism of fluorosilane condensation onto a surface.

Scanning electron microscopy

The rough surface of NyCo fabric was examined with a scanning electron microscope (SEM, Hitachi S-3200 N) operated at 5 and 10 kV and magnifications from ×25 to ×10,000. Revolution™ v1.60b24 (4pi Analysis Inc.) was used for image analysis of SEM images. On a rough surface, the fiber diameters and the distances among adjacent fibers were measured using this program.

Contact angle measurements

The contact angles of water and dodecane on the prepared surfaces were measured from sessile water drops using a lab-designed goniometer at 20 °C. The volumes of the deposited droplets were 2, 5, and 10 μL. The range of contact angles were obtained from at least three individual measurements each on a new spot. The image of liquid droplets on the prepared surface has been obtained using a digital camera (Cannon EOS EF-S-18-55IS) having an optical microscopic focusing lenses (Meiji Techno EMZ-13TR).
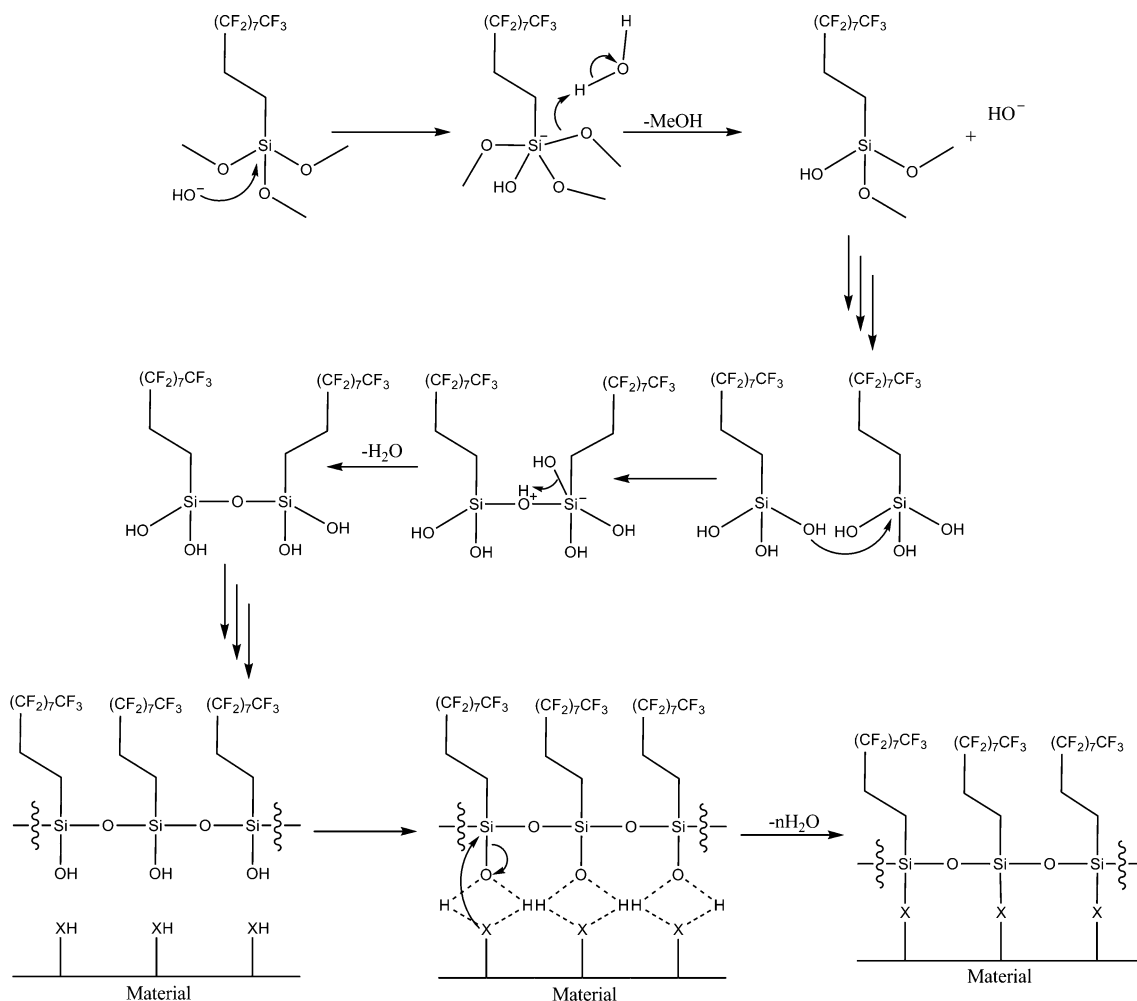
Scheme 1 Reaction mechanism of fluorosilane condensation onto a surface

Results and discussion

Since the wetting behavior of a solid surface is controlled by the chemical composition and the geometrical structure of the surface, we used a two stage procedure to form a superhydrophobic ultraoleophobic NyCo surface. We chemically modified NyCo to generate a low-surface-tension surface and roughened the NyCo surface to provide a proper morphology and roughness. First, we verify that the chemical procedure described in "Experimental" results in a low-surface-energy when the fluorosilane is grafted onto the substrate.

Chemical modification

We chemically grafted fluorosilane onto a NyCo surface to reduce the surface tension of NyCo and to make the surface *less oleophilic*. Meanwhile, in order to obtain the Young contact angles, θ_e, of water and dodecane, nylon 6,6 film was treated with fluorosilane. The water contact angles, $\theta_{e\text{-water}}$, on a fluorosilane-grafted nylon film were 109°–112°, while $\theta_{e\text{-water}}$ on an unmodified nylon surface were 70°–73°. Grafting fluorosilane to a nylon film also increased dodecane contact angles. The dodecane contact angles, $\theta_{e\text{-dodecane}}$, on fluorosilane-grafted nylon film were 73°–75°, while $\theta_{e\text{-dodecane}}$ on an unmodified nylon surface was <5°. The measured values of $\theta_{e\text{-water}}$ and $\theta_{e\text{-dodecane}}$ on fluorosilane-treated nylon are such important parameters to design an ultraoleophobic surface using the Wenzel and the Cassie–Baxter models. Fluorosilane grafted onto nylon 6,6 successfully generated a surface having low-surface-tension.

Geometrical modification

Again, to form a superhydrophobic ultraoleophobic surface, the surface must have a low-surface-tension and proper roughness. In the Cassie–Baxter model, a liquid sits on a composite surface made of two different materials: a solid and air. In this approach a contact angle at a rough surface can be described as:

$$\cos \theta_r^{CB} = f_1 \cos \theta_e - f_2 \tag{2}$$

where $\cos\theta_r^{CB}$ is an apparent contact angle on a Cassie–Baxter surface, f_1 is the surface area of the liquid in contact with solid divided by the projected area, and f_2 is the surface area of the liquid in contact with air divided by the projected area [18]. Simply, Eq. 2 can be regarded as an advanced Wenzel model, presenting a rough surface having air in a rough structure. That is if $f_2 = 0$ in Eq. 2, the rough surface becomes completely wet. Wenzel proposed the following equation before Cassie and Baxter had developed Eq. 2.

$$\cos \theta_r^W = r \cos \theta_e \tag{3}$$

where θ_r^W is an apparent contact angle on a Wenzel surface, and r is the ratio of the total wet area of a rough surface to the apparent surface area in contact with the water droplet [19]. Here, r is equal to f_1 in Eq. 2. According to Eq. 3, for a material with a smooth surface having $109° \leq \theta_{\text{e-water}} \leq 112°$ and $73° \leq \theta_{\text{e-dodecane}} \leq 75°$, r must be greater than 2.66 to make the surface superhydrophobic, but the surface cannot be oleophobic since this rough surface will become wet no matter how long it takes. The combination of Eqs. 2 and 3 reinforces the concept of the metastable Cassie–Baxter model. A surface having $\theta_e < 90°$ will become immediately wet (the Wenzel model), or eventually wet unless the force of drag caused by the solid, air pockets, the cohesive energy of liquid, etc. is greater than gravity (the metastable Cassie–Baxter model). Therefore, we design a woven twill fabric having $r > 2.66$ to create a metastable Cassie–Baxter surface.

Figure 1 shows a cross-sectional view of a model of a NyCo twill woven fabric made of monofilament fibers. The surface area of a single round monofilament fiber in the unit fabric can be calculated using flux integral. The distance from the center of a weft (or warp) yarn to the center of an adjacent weft (or warp) yarn is $4R$, and the distance from the center of a weft (warp) yarn to the center of an adjacent warp (weft) yarn is $2R$. Hence, the vector from the center of one weft yarn to the center of an adjacent weft yarn, or the vector from the center of one warp yarn to the center of an adjacent warp yarn, makes a $30°$ angle to the plane of the fabric. Meanwhile, the area of one yarn in the unit fabric is:

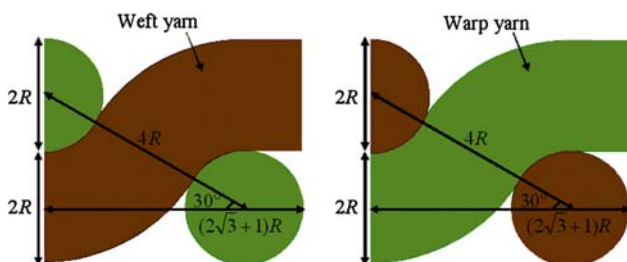Fig. 1 Cross-sectional views of a twill woven fabric

$$r(u,v) = (2R + R\cos v)\cos u\, i + (2R + R\cos v)\sin u\, j + R\cos v\, k$$

$$r_u = -(2R + R\cos v)\sin u\, i + (2R + R\cos v)\cos u\, j$$

$$r_v = -R\sin v\cos u\, i - R\sin v\sin u\, j + R\cos v\, k$$

$$r_u \times r_v = R(2R + R\cos v)\cos u\cos v\, i \\ + R(2R + R\cos v)\sin u\cos v\, j \\ + R(2R + R\cos v)\sin v\, k$$

$$|r_u \times r_v| = R(2R + R\cos v)$$

$$A_{\text{yarn in unit area}} = \frac{\int_0^{2\pi}\int_0^{2\pi} R(2R + R\cos v)\,du\,dv}{3} + \frac{\pi R^2}{2}$$
$$= \left(\frac{8\pi^2}{3} + \frac{\pi}{2}\right)R^2 \tag{4}$$

The area of one yarn in the unit fabric is applied to both weft and warp yarns, and a twill fabric in Fig. 1 consists of four yarns in the unit area. Therefore, the real fabric area is:

$$A_{\text{fabric}}^{\text{real}} = 4\left(\frac{8\pi^2}{3} + \frac{\pi}{2}\right)R^2 = 111.56R^2 \tag{5}$$

where $A_{\text{fabric}}^{\text{real}}$ is the intrinsic area of the unit fabric determined by the area of yarn surfaces. The apparent surface area is equal to the area of a plane tangent to the top surface.

$$A_{\text{fabric}}^{\text{apparent}} = \left[R(2\sqrt{3} + 1)\right]^2 = 19.93R^2 \tag{6}$$

where $A_{\text{fabric}}^{\text{apparent}}$ is the apparent area of the unit fabric shown in Fig. 1. Finally, the roughness, r, is the ratio of these areas:

$$r = \frac{A_{\text{fabric}}^{\text{real}}}{A_{\text{fabric}}^{\text{apparent}}} = \frac{111.56R^2}{19.93R^2} = 5.59 \tag{7}$$

If this twill woven fabric is made of yarns having multifilament fibers as shown in Fig. 2, the fabric will have even higher values of roughness and $r > 5.59$, since the space between the fibers will increase the intrinsic surface area while the apparent surface area remains the same. Therefore, the twill woven rough surface has high enough r to be a metastable Cassie–Baxter surface regardless of the structure of yarns.

Now, we model a Cassie–Baxter twill woven fabric. In Fig. 1, the center-to-center distance is $(2\sqrt{3} + 1)R$. Thus, f_1 and f_2 are:

$$f_1 = \frac{4(\pi - \theta_e) + 1}{2\sqrt{3} + 1}$$

$$f_2 = 1 - \frac{1 + 4\sin\theta_e}{2\sqrt{3} + 1}$$

Substituting f_1 and f_2 to Eq. 2, a Cassie–Baxter NyCo surface is defined as:
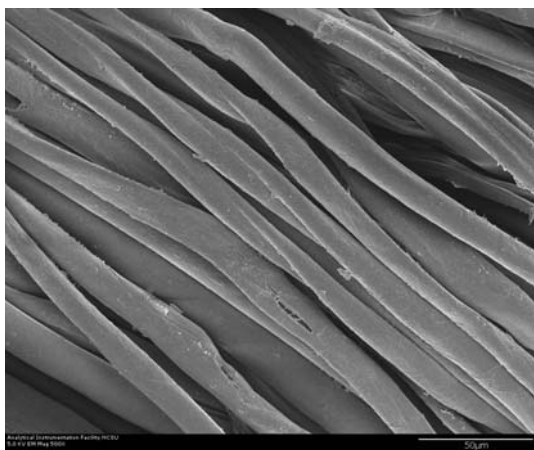
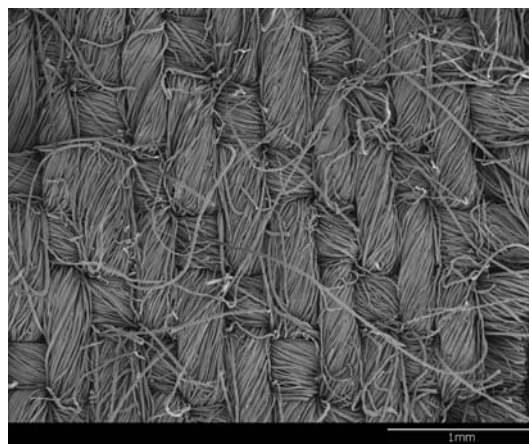**Fig. 2** SEM micrograph of a NyCo multifilament yarn (×500)

Fig. 3 SEM micrograph of a multifilament twill woven fabric (×25)

$$\cos \theta_r^{CB} = \frac{4(\pi - \theta_e) + 1}{2\sqrt{3} + 1} \cos \theta_e + \frac{1 + 4\sin \theta_e}{2\sqrt{3} + 1} - 1 \qquad (8)$$

Substituting Young contact angles into Eq. 8 along with the measured contact angles from the flat nylon film provides θ_r^{CB}. As a numerical example, we obtain $111° \le \theta_{r\text{-water}}^{CB} \le 115°$ by substituting the Young contact angles of water on a fluorosilane-treated nylon film, $109° \le \theta_{e\text{-water}} \le 112°$, into Eq. 8. However, neither $109° \le \theta_{e\text{-water}} \le 112°$ nor $73° \le \theta_{e\text{-dodecane}} \le 75°$, which are measured Young contact angles, can be used for the prediction of apparent contact angles on a rough surface shown in Fig. 1 because f_2 must be greater than 0 in the Cassie–Baxter model. For $f_2 \ge 0$ in Eq. 8, $\theta_e \ge 120°$. Since both $\theta_{e\text{-water}}$ and $\theta_{e\text{-dodecane}}$ are the measured values and cannot be changed, the twill woven fabric needs to be geometrically modified to be a Cassie–Baxter surface. Therefore, as the next step, we model a twill woven fabric having yarns made of multifilament fibers.

Figure 2 shows a yarn made of multifilament fibers. We begin by determining the apparent contact angle of the liquid with this yarn. From Fig. 2, it is seen that the fiber spacing is approximately equal to the fiber diameter, i.e. $d \sim R_f$, where R_f is the fiber radius and d is the distance between two adjacent fibers. Substituting R_f for R and d into the following Eq. 6 in our previous research [20]:

$$\cos \theta_r^{CB} = \frac{R_f}{R_f + d}(\pi - \theta_e)\cos \theta_e + \frac{R_f}{R_f + d}\sin \theta_e - 1$$

Equation 9 is obtained as:

$$\cos \theta_r^{multifilament} = \frac{\pi - \theta_e}{2}\cos \theta_e + \frac{\sin \theta_e}{2} - 1 \qquad (9)$$

Substituting $109° \le \theta_{e\text{-water}} \le 112°$ and $73° \le \theta_{e\text{-dodecane}} \le 75°$ into Eq. 9, we find $137° \le \theta_{r\text{-water}}^{CB} \le 139°$ and $104° \le \theta_{r\text{-dodecane}}^{CB} \le 106°$ for the fluorosilane-grafted multi-filaments. Using these values as the effective contact angles

for the yarns in the woven structure and re-solving Eq. 8, i.e., substituting these values into $\theta_{e\text{-water}}$ and $\theta_{e\text{-dodecane}}$ in Eq. 8, we predict $145° \le \theta_{r\text{-water}}^{CB} \le 147°$ and $104° \le \theta_{r\text{-dodecane}}^{CB} \le 107°$ for the fluorosilane-grafted multifilament twill woven fabric which is shown in Fig. 3. According to our prediction, NyCo multifilament twill woven fabric can be neither superhydrophobic nor ultraoleophobic by itself even if the fabric is treated with a low-surface-tension chemical. In order to achieve superhydrophobicity and ultraoleophobicity, the fabric morphology has to be manipulated by creating bigger spaces between fibers, loosening the fabric structure, or providing more roughness to the surface of NyCo multifilament fibers. Considering the manufacturing process of woven fabrics, providing more roughness by coating protuberances on the surface of NyCo fibers seems to be the easiest way to achieve superhydrophobicity and ultraoleophobicity. When the NyCo multifilament surface is covered with protuberances in micro and nano sizes, a model surface shown in Fig. 4 are obtained.

Based on the model in Fig. 4, a Cassie–Baxter equation on this surface is defined as:

$$\cos \theta_r^{particles} = \frac{R_p}{R_p + d_p}(\pi - \theta_e)\cos \theta_e + \frac{R_p}{R_p + d_p}\sin \theta_e - 1 \qquad (10)$$
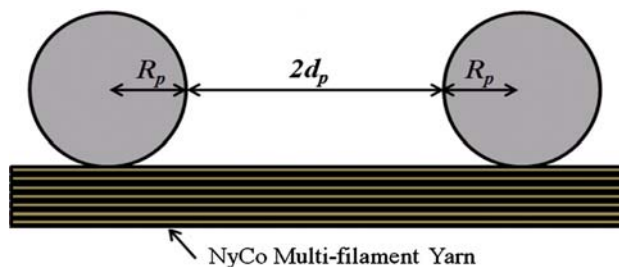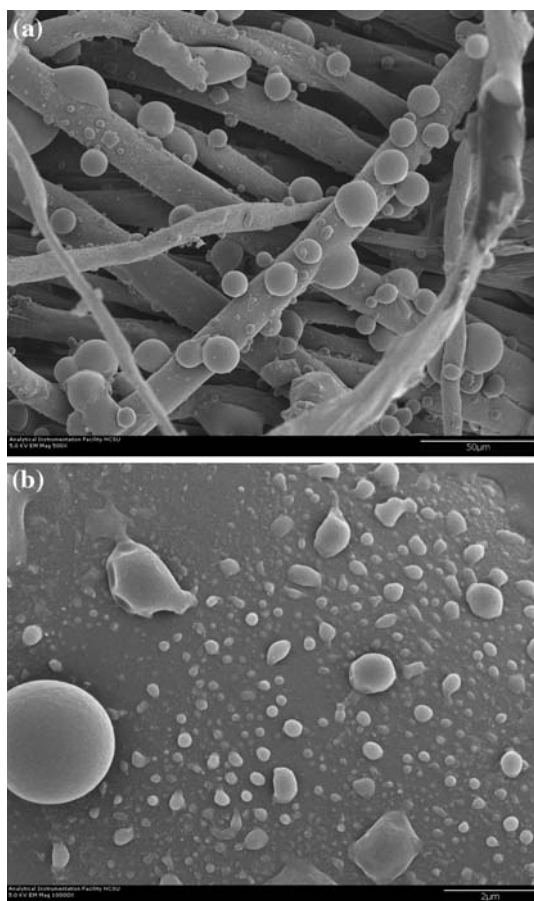

Fig. 4 Two adjacent protuberances on a NyCo surface

Fig. 5 SEM micrographs of fluorosilane-treated on NyCo **a** ×500 and **b** ×10,000

where R_p is the radius of the protuberances on a NyCo substrate and $2d_p$ is the distance between two adjacent protuberances. The SEM images of fluorosilane-grafted NyCo multifilament twill woven fabric having micro and nano protuberances are shown in Fig. 5; R_p and $2d_p$ are varied from 50 nm to 20 μm and 300 nm to 200 μm, respectively. Substituting $\theta_{e\text{-water}}$, $\theta_{e\text{-dodecane}}$, R_p, and $2d_p$ from the SEM images into Eq. 10, we find $\cos\theta_r^{particles}$ which is substituted into θ_e in Eq. 9. In the same manner, $\cos\theta_r^{multifilament}$ obtained from Eq. 9 are substituted into θ_e in Eq. 8. Finally, we find $\theta_{r\text{-water}}^{CB} \sim 180°$ and $147° \leq$

$\theta_{r\text{-dodecane}}^{CB} \leq 151°$. The predicted values are in good agreement with the measured angles which vary $168° \leq \theta_{r\text{-water}}^{CB} \leq 175°$ and $151° \leq \theta_{r\text{-dodecane}}^{CB} \leq 155°$. Figure 6 shows water and dodecane droplets on the surface shown in Fig. 5; the initial apparent contact angles of water and dodecane in Fig. 6 are 170° and 151°, respectively; and both droplets are sitting on top of the rough surface. However, dodecane is slowly drawn into the woven structure with reducing $\theta_{r\text{-dodecane}}^{CB}$ while water stays on top of the surface until water completely evaporates. For example a 10 μL water droplet evaporates in 30 min, but a dodecane droplet stays on top of the surface over 1 h without changing $\theta_{r\text{-dodecane}}^{CB}$. Then, $\theta_{r\text{-dodecane}}^{CB}$ steadily decreases since dodecane penetrates the rough surface. These phenomena well describe the wetting behavior of stable and metastable Cassie–Baxter surfaces. If $\theta_e > 90°$, a liquid sitting on top of the surface stays until it evaporates since air pockets beneath a droplet leads to a Cassie–Baxter surface. However, if $\theta_e < 90°$, a liquid contacting with a rough surface can sit on top of the surface for a certain amount of time due to the minimization of surface energy caused by trapped air underneath the droplet. Then, the liquid begins to penetrate the rough surface in the process of thermodynamic equilibrium. An ultraoleophobic surface can be created by designing a metastable Cassie–Baxter surface while a superhydrophobic surface can be produced by creating a Cassie–Baxter surface. Therefore, not only chemical treatment reducing surface energy but also geometrical modification increasing robustness is required to design a durable ultraoleophobic surface.

Conclusion

A superhydrophobic ultraoleophobic surface is obtained by two criteria: a low-surface-tension and a properly designed rough surface having appropriate surface roughness and morphology. In order to make NyCo superhydrophobic and ultraoleophobic, NyCo multifilament twill woven fabric was treated with fluorosilane which has a very low-surface-tension and provides more roughness to the fabric by generating protuberances in the form of fluorosilane

Fig. 6 Water and dodecane droplets on a NyCo fabric
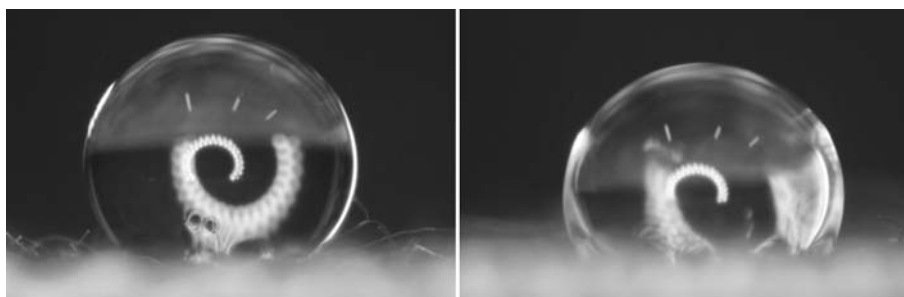
condensates on the fiber surfaces. From the Young contact angles of water and dodecane on a fluorosilane-grafted nylon film, we predicted the apparent contact angles on a fluorosilane-grafted NyCo multifilament twill woven fabric. Good agreement between the predicted values and the observed contact angles was obtained. On our superhydrophobic rough surface, water contact angles were as high as 175° while apparent dodecane contact angles were as high as 155°. Dodecane was slowly drawn into the fabric with a reduction the apparent contact angle, while water remained on top of the surface until completely evaporating. An ultraoleophobic surface has been created by designing a metastable Cassie–Baxter rough surface.

References

1. Cai Y, Li Q, Wei Q, Wu Y, Song L, Hu Y (2008) J Mater Sci 43:6132. doi:10.1007/s10853-008-2921-6
2. Lee B, Dai G (2009) J Mater Sci 44:4848. doi:10.1007/s10853-009-3739-6
3. Pascual M, Balart R, Sanchez L, Fenollar O, Calvo O (2008) J Mater Sci 43:4901. doi:10.1007/s10853-008-2712-0
4. Berketis K, Tzetzis D (2009) J Mater Sci 44:3578. doi:10.1007/s10853-009-3485-9s
5. Huang X, Fang X, Lu Z, Chen S (2009) J Mater Sci 44:4522. doi:10.1007/s10853-009-3660-z
6. Lee HJ (2009) J Mater Sci 44:4645. doi:10.1007/s10853-009-3711-5
7. Mueller-Plathe F, Pal S, Weiss H, Keller H (2005) Soft Mater 3:21
8. Hoefnagels HF, Wu D, de With G, Ming W (2007) Langmuir 23:13158
9. Brewer SA, Willis CR (2008) Appl Surf Sci 254:6450
10. Ahuja A, Taylor JA, Lifton V, Sidorenko AA, Salamon TR, Lobaton EJ, Kolodner P, Krupenkin TN (2008) Langmuir 24:9
11. Lee HJ, Willis C (2009) Chem Ind 21
12. Tuteja A, Choi W, Ma M, Mabry JM, Mazzella SA, Rutledge GC, McKinley GH, Cohen RE (2007) Science 318:1618
13. Lee HJ, Michielsen S (2007) J Polym Sci B 45:253
14. Tuteja A, Choi W, Mabry JM, McKinley GH, Cohen RE (2008) Proc Natl Acad Sci 105:18200
15. Leng B, Shao Z, de With G, Ming W (2009) Langmuir 25:2456
16. Steele A, Bayer I, Loth E (2009) Nano Lett 9:501
17. Lee HJ, Michielsen S (2006) J Text Inst 97:455
18. Cassie ABD, Baxter S (1944) Trans Faraday Soc 40:546
19. Wenzel RN (1936) Ind Eng Chem 28:988
20. Michielsen S, Lee HJ (2007) Langmuir 23:6004